RAPID COMMUNICATIONS

PHYSICAL REVIEW B **90**, 140204(R) (2014)

Identification of relaxing structural defects in densified B_2O_3 glasses

Giovanni Carini Jr.,[1] Giuseppe Carini,[2] Giovanna D'Angelo,[2] Daniele Fioretto,[3] and Gaspare Tripodo[2]
[1]*IPCF del C.N.R., U.O.S. di Messina, I-98158 Messina, Italy*
[2]*Dipartimento di Fisica e Scienze della Terra, Università di Messina, I-98166 Messina, Italy*
[3]*Dipartimento di Fisica e Geologia, Università di Perugia, I-06123 Perugia, Italy*

(Received 7 February 2014; revised manuscript received 30 September 2014; published 28 October 2014)

Sound propagation has been investigated at megahertz and gigahertz frequencies in B_2O_3 solids which have been pressure quenched to go through different glassy phases having growing density until the crystalline state. Over the temperature range between 10 and 300 K, the attenuation and velocity of sound in glasses are regulated by classical activation over potential barriers of structural defects and vibrational anharmonicity. The defect states are absent in the crystalline phase whose acoustic behavior is determined only by the anharmonic coupling between sound waves and thermal vibrations. Our study leads to identification of the specific superstructural units subjected to thermally activated motions in vitreous B_2O_3. These molecular groups are the boroxol rings which are formed due to the poor atomic packing of glassy networks and are missing in the crystal.

DOI: 10.1103/PhysRevB.90.140204 PACS number(s): 63.50.Gh, 62.40.+i, 62.65.+k, 62.80.+f

Local motions (tunneling and relaxation) of intrinsic structural defects, in addition to the vibrational anharmonicity, regulate the attenuation and velocity of sound in oxide glasses below room temperature over the wide frequency range, from kilohertz to gigahertz [1–5]. Low-energy defect states cause attenuation peaks and related dispersion in the sound velocity, while the anharmonicity, determined by the "thermal vibration viscosity," becomes prevalent in determining the sound dissipation in the gigahertz region [4,5]. Some exception to this general trend is offered from the sound velocity behavior in tetrahedrically bonded glasses, which reveal an anomalous, poorly understood hardening also at temperatures well below room temperature [4]. The nature of defect states in glasses has remained elusive, in spite of experimental and theoretical efforts made over many years [6], mainly because the amorphous structure is not well understood beyond the short-range order, even for simple prototype oxide glasses. The structural origin of defect states can be explored by glass densification, because it leads to significant modifications of the short- and medium-range orders [7,8] and to a reduction of the local atomic mobility [9] without altering the stoichiometry. In fact, growing densification of vitreous boron oxide (v-B_2O_3), whose network is made up of three connected planar BO_3 triangles and boroxol rings (B_3O_6, the superstructural units formed by three corner-sharing BO_3 triangles [10]), leads to the progressive decrease of rings and the formation of tetra-coordinated boron atoms. In addition to this, by comparing normal and compacted glasses of SiO_2 with its different crystalline polymorphs having growing density, Chumakov *et al.* [11] showed that the excess "glassy" vibrational density of states (e.g., the "boson peak") is a stronger function of the density of the material than of its atomic disorder.

To follow the correlation between intrinsic defect states and the structural changes without modification of the chemical bonding, we have performed ultrasonic and hypersonic (Brillouin light scattering, BLS) experiments on samples of B_2O_3, which have been high-pressure quenched to go through different glassy phases having growing density to the crystalline state. The results evidence that the decrease of boroxol rings with increasing pressure of synthesis leads to the progressive depression of relaxation processes until their full disappearance in the crystalline phase, where the rings are missing.

Two different samples, obtained by quenching melts of $^{11}B_2O_3$ under a pressure of 4 GPa, are studied: 4-GPa/B3 glass and a polycrystalline sample, c-B_2O_3. Details of these samples have been given in a previous publication [12]. 4-GPa/B3 glass is structurally different from that previously synthesized at 4 GPa (4-GPa/B4 glass) but at higher temperatures [8], which revealed the formation of fourfold-coordinated boron atoms. As detailed in the following, the former is characterized by no variation of the chemical bonding and by a lower density than the latter (at room temperature, $\rho = 2174\ \mathrm{kg/m^3}$ for 4-GPa/B3 glass and $\rho = 2373\ \mathrm{kg/m^3}$ for 4-GPa/B4 glass).

The Raman spectra and the attenuation and velocity of 10-MHz ultrasounds were measured using the same procedures elsewhere described [8,9]. The short length of c-B_2O_3 prevented a reliable measurement of the very high sound velocity. In this case, the velocities of longitudinal (V_l) and shear (V_t) waves were determined by measuring the frequency shifts, $\nu_{B,i} = \frac{2nV_i}{\lambda_L}\sin(\frac{\theta}{2})$, of transverse (TA) and longitudinal (LA) acoustic modes observed in BLS spectra [13] with a refraction index $n = 1.61$ [14]. A polycrystalline sample is an inhomogeneous solid because one elastically anisotropic grain is different from all those around it. This basic inhomogeneity within the scattering volume causes a parasitic broadening of Brillouin lines which prevents any accurate evaluation of the intrinsic linewidth Γ and the related sound attenuation determined by physical mechanisms [4,5]. In addition to this, the progressively growing weakness of TA mode lines with decreasing temperature below room temperature also prevented an acceptable evaluation of the frequency shift $\nu_{B,t}$. Due to the above reasons, the low-temperature measurements in c-B_2O_3 are restricted here to the frequency shift $\nu_{B,l}$ of the LA mode. The room-temperature Debye sound velocities $V_D(\frac{3}{V_D^3} = \frac{1}{V_l^3} + \frac{2}{V_t^3})$ are $V_l = 5287$ m/s, $V_t = 3021$ m/s, $V_D = 3357$ m/s (4-GPa/B3 glass); $V_l = 8344$ m/s, $V_t = 4069$ m/s, $V_D = 4571$ m/s (c-B_2O_3).

The room-temperature Raman spectra of 4-GPa/B3 and 4-GPa/B4 glasses between 600 and 1600 $\mathrm{cm^{-1}}$ are compared in Fig. 1 for VV (polarized) configuration. The intensities have

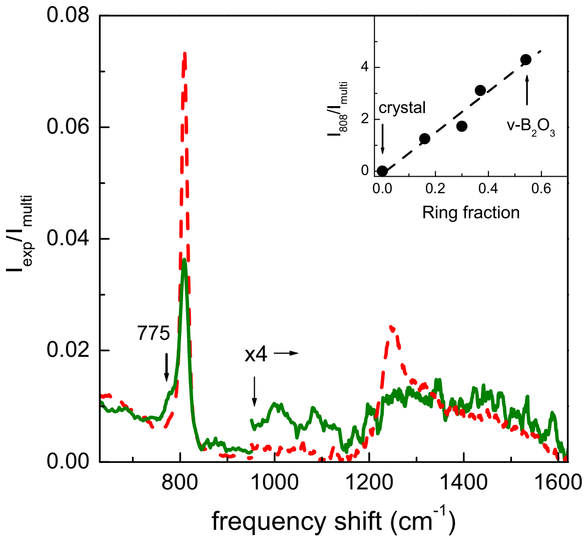

FIG. 1. (Color online) Experimental Raman intensities (VV polarization) above 600 cm^{-1} normalized by the integrated intensity of the multiband between 1200 and 1600 cm^{-1} of 4-GPa/B3 (dashed line) and 4-GPa/B4 (solid line) glasses; the region above 950 cm^{-1} is reported with a y scale expanded by a factor of 4. Inset shows the normalized integrated intensities of the band at 808 cm^{-1} vs the boroxol ring fraction as determined by NMR data [from Ref. 7] in B_2O_3 glasses.

been normalized by the total integrated intensity I_{multi} of the multicomponent band between 1200 and 1600 cm^{-1}, which is determined by vibrations of all the units forming the whole glassy network [8]. The intense and highly polarized line at 808 cm^{-1} arises from a localized breathing-type vibration of oxygen atoms inside the boroxol rings. Densification decreases the intensity I_{808} of this band but preserving its frequency. In 4-GPa/B4 glass, there is a further band at 775 cm^{-1} due to vibrations of superstructural units containing tetrahedral BO_4 groups, the pentaborate units, a feature which implies changes in the chemical bonding characterizing the network [8]. Quite differently, 4-GPa/B3 glass preserves the shape of the I_{808} band observed in v-B_2O_3, a feature indicating no variation of boron coordination. The same short-range order characterizes the networks of both these glasses, the only modifications due to densification arising from changes of the medium-range order which give rise to the reduction of I_{808} associated to the progressive decrease of the ring population [12]. The inset of Fig. 1 reports the integrated intensity of the band at 808 cm^{-1} normalized by I_{multi} vs the ring fraction determined by NMR data in B_2O_3 glasses, which have been compacted to go through different glassy phases having growing density [7]. The plot reveals a strikingly linear increase of I_{808}/I_{multi} with increasing ring fraction starting from the crystalline structure where boroxol rings are fully missing [15]. The lattice of the crystal, in fact, is made up of interconnected ribbons of BO_3 triangles with each oxygen atom bridging between two boron atoms; no band at 808 cm^{-1} is observed in the crystal, an unquestionable evidence of the absence of boroxol rings [12].

Figure 2(a) compares the temperature behavior of the internal friction Q^{-1} [16] in 4-GPa/B3 glass with data recently obtained in v-B_2O_3 and 2-GPa glass [9]. The broad loss peak, observed at about 73 K in v-B_2O_3 and arising from thermally activated relaxations of structural defects, is reduced by a factor of 3 and shifted to about 63 K in 4-GPa/B3 glass. In Fig. 2(b), the relative change $\frac{\Delta V}{V_0} = \frac{V(T)-V_0}{V_0}$ of the shear sound velocity is shown as a function of temperature, V_0 being the sound velocity at the lowest temperature in the experiment. The sound velocity shows a negative temperature coefficient over the whole investigated range in all the glasses, but decreasing much steeper between 8 and 120 K. In c-B_2O_3, the velocity of 50-GHz longitudinal sound waves exhibits only a gradual decrease with increasing temperature. The behavior observed in glasses below 120 K is understood in terms of the relaxation processes discussed above for the internal friction, while the nearly linear decrease at higher temperatures is due to the vibrational anharmonicity [9]. As for the acoustic loss, increasing compaction reduces the slope in $(\frac{\Delta V}{V_0})$ below 120 K, which is a measure of the relaxation strength. No relaxation contribution is revealed in c-B_2O_3, whose velocity behavior appears to be regulated only by vibrational anharmonicity. We like to note that we use the velocity measurements for the

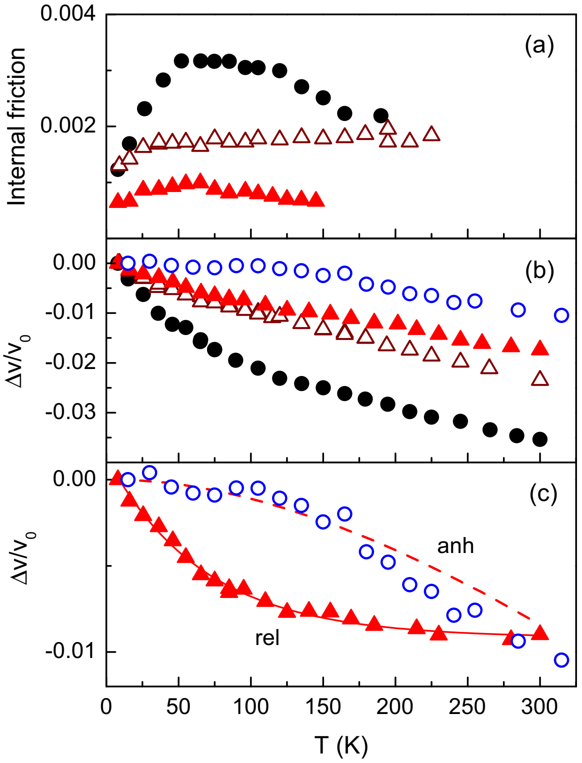

FIG. 2. (Color online) (a) Temperature dependences of the internal friction Q^{-1} of 10-MHz shear waves in v-B_2O_3 (●), 2-GPa glass (△), and 4-GPa/B3 glass (▲). (b) Temperature dependences of the fractional sound velocities, $\frac{\Delta V}{V_0} = \frac{V(T)-V_0}{V_0}$, of 10-MHz shear waves in v-B_2O_3 (●), 2-GPa glass (△), 4-GPa/B3 glass (▲), and of 50-GHz longitudinal acoustic waves in c-B_2O_3 (○). (c) Anharmonic [dashed line, evaluated by Eq. (2)] and relaxation (▲, obtained by difference between the experimental data and the anharmonic behavior) contributions to the fractional sound velocity in 4-GPa/B3 glass. Solid line represents the fit to the relaxation curve by Eq. (1). The data measured in c-B_2O_3 are also included for comparison (open circles).

following analysis because they are much more accurate than those of internal friction.

Relaxation and anharmonic mechanisms can be well described by the asymmetric double-well potential (ADWP) model [17] and Akhiezer's or *phonon viscosity* theory [18], respectively. In the former, local defects subjected to thermally activated motions within asymmetric double-well potentials, having broad distributions of both the barrier height W and the asymmetry Δ, are considered. Using for $g(W)$ an exponential form, $g(W) = W_0^{-1}\exp(-\frac{W}{W_0})$, and taking $f(\Delta)$ as a constant f_0, the internal friction and the dispersion can be expressed by the following relations [19]:

$$\begin{aligned} Q_{\rm rel}^{-1} &= 2C^*\left[\frac{\alpha\pi/2}{\cos(\alpha\pi/2)}y_0^{\alpha} - \frac{\alpha}{1-\alpha}y_0\right], \\ \left(\frac{\Delta V}{V_0}\right)_{\rm rel} &= C^*\left[\frac{\alpha\pi/2}{\sin(\alpha\pi/2)}y_0^{\alpha} - 1\right], \end{aligned} \tag{1}$$

where $\alpha = \frac{k_B T}{W_0}$ and $y_0 = \omega\tau_0$, τ_0 being a constant related to the relaxation time. The relaxation strength is given by $C^* = \frac{\gamma^2 f_0}{\rho V^2}$, γ being the deformation potential that expresses the coupling between the ultrasonic stress and the two-well systems.

The anharmonic contribution can be assessed by extending to glasses the Akhiezer mechanism of phonon viscosity [18,20], which describes the interaction of sound waves with thermal phonons in dielectric crystals at high temperatures, where the mean free path of thermal modes is shorter than the acoustic wavelength. Assuming a single value for the mean lifetime of thermal vibrations $\tau_{\rm th}$, the acoustic loss and the variation of the sound velocity are given by [4,5]

$$\begin{aligned} Q_{\rm anh}^{-1} &= A(T)\omega\tau_{\rm th}, \\ \left(\frac{\Delta V}{V_0}\right)_{\rm anh} &= -\frac{1}{2}\frac{\gamma_G^2 C_V T V}{2\rho V_D^3} = -\frac{A(T)}{2}, \end{aligned} \tag{2}$$

where γ_G^2 is the mean-squared average Grüneisen parameter for the thermal modes, C_V the specific heat per unit volume, and V_D the Debye velocity. Quite interestingly, $(\frac{\Delta V}{V_0})_{\rm anh}$ predicts a nearly linear temperature decrease for the sound velocity, as usually observed in glasses which do not have a tetrahedrically coordinated network [2,3,21].

Evaluation of the relaxation and anharmonic contributions to the sound velocity in 4-GPa/B3 glass has been performed by Eqs. (1) and (2), applying the same procedure previously proposed [9]. The temperature behavior of $(\frac{\Delta V_t}{V_{t,0}})_{\rm anh}$ is reported as a dotted line in Fig. 2(c), while the fit of $(\frac{\Delta V_t}{V_{t,0}})_{\rm rel}$ by Eq. (1) as a solid line. The experimental data of $(\frac{\Delta V_l}{V_{l,0}})$ for c-B_2O_3, also reported in the same figure, show that the sound velocity behavior in the crystal is fully controlled by the vibrational anharmonicity arising from the lattice viscosity. The values of γ_G^2 and of the relaxation parameters are $\gamma_G^2 = 1.56$, $C^* = 0.00917$, $W_0/k_B = 676$ K, $\tau_0 = 6.9 \times 10^{-13}$ s, for 4-GPa/B3 glass; $\gamma_G^2 = 1.84$ for c-B_2O_3.

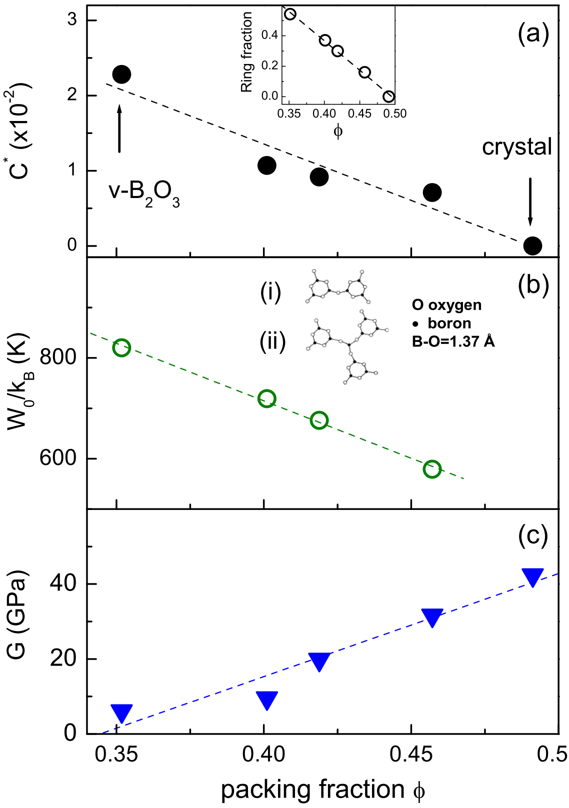

FIG. 3. (Color online) Behaviors of (a) the relaxation strength C^*, (b) the average activation energy W_0/k_B, and (c) the shear modulus G vs the atomic packing fraction ϕ. Inset of (a) shows the boroxol ring fraction vs ϕ and inset of (b) the schematic illustration of planar boroxol rings (B_3O_6) connected by (i) a single bridging oxygen or (ii) a BO_3 triangular unit. The approximate B-O interatomic distance is given in angstroms. The dashed lines are linear data fits.

The data reported in Figs. 3(a) and 3(b), also including results previously obtained in 2-GPa and 4-GPa/B4 glasses [9], show that both the relaxation strength C^* and the apparent activation energy W_0 decrease with the increasing packing fraction ϕ. Atomic packing changes from 0.35 in v-B_2O_3 to 0.49 in c-B_2O_3 [12] and determines a straightforward linear decrease of the boroxol ring population [see inset of Fig. 3(a)]. The reduction of the average activation energy W_0 implies that network compaction leads to the gradual disappearance of relaxing systems with higher barriers. More importantly, the relaxation strength C^* decreases linearly from 2.28×10^{-2} in v-B_2O_3 down to zero in c-B_2O_3 where relaxations are totally absent. Since extrinsic defects, such as OH^- groups, can be excluded as the origin of relaxation processes observed in these glasses [9], the progressive decrease of C^* must be attributed to a parallel reduction of intrinsic defects, i.e., relaxing structural units which must be missing in the crystal. In addition to this, Fig. 3(c) shows that growing packing leads to a linear increase of the shear modulus G $(=\rho V_t^2)$, which becomes up to a factor of 7 higher than that of v-B_2O_3. As boroxols decrease linearly with increasing packing up to the crystal containing no ring, the present observations lead us to associate the hardening of glasses to the progressive decrease of ring population and the relaxations affecting the sound propagation to thermally activated local motions of linked rings, these superstructural units having no internal degrees of freedom in terms of variable bond or torsion angles [10]. The rings can be connected either by a single oxygen atom bridging two rings or by one or several planar BO_3 triangles [22] [inset of Fig. 3(b)], the latter configuration being representative of relaxors with higher potential barriers as a consequence of more limited degrees of freedom. The formation of ring bridging via BO_3 triangles needs a larger volume than the formers and is surely prevented with increasing densification. The restriction imposed by the progressively increasing packing should result in rings mainly connected via a single bridging oxygen, whose local movements are characterized by smaller potential barriers. The overall result of these structural changes should be a decrease of W_0, as observed.

The existence of unknown structural units making up the glassy network and subjected to thermally activated relaxations, which strongly depend on the chemical composition, is a very general topic [6,23]. The acoustic behavior of crystalline quartz is regulated by anharmonicity *via phonon viscosity* [24], while relaxation processes dominate the sound attenuation and velocity in vitreous silica over the same frequency and temperature regions [4] and are strongly depressed by densification [25]. Glassy B_2O_3 was specifically chosen in this work as a model system in which densification and the joint investigation by means of different experimental techniques allowed us to identify the structures responsible for the medium-range relaxation. This result opens the hunt for similar structures in a myriad of amorphous solids, such as inorganic and organic glasses where the sound propagation was widely studied but poorly understood. It is concluded that relaxations of intrinsic defects dictating the universal behavior of the sound propagation in glasses originate from specific *glassy* units which are the building blocks of the medium-range order of the network. In vitreous B_2O_3, these superstructural groups are the boroxol rings which are fully missing in the crystal.

---

[1] S. Rau, C. Enss, S. Hunklinger, P. Neu, and A. Würger, Phys. Rev. B **52**, 7179 (1995).

[2] G. Carini, Jr., G. Carini, G. D'Angelo, G. Tripodo, A. Bartolotta, and G. Salvato, Phys. Rev. B **72**, 014201 (2005).

[3] G. Carini, Jr., G. Carini, G. D'Angelo, G. Tripodo, A. Bartolotta, and G. Di Marco, J. Phys. Cond. Matter **18**, 10915 (2006).

[4] R. Vacher, E. Courtens, and M. Foret, Phys. Rev. B **72**, 214205 (2005).

[5] G. Carini, Jr., G. Tripodo, and L. Borjesson, Phys. Rev. B **78**, 024104 (2008).

[6] R. Pohl, X. Liu, and E. Thompson, Rev. Mod. Phys. **74**, 991 (2002).

[7] V. V. Brazhkin, I. Farnan, K.-I. Funakoshi, M. Kanzaki, Y. Katayama, A. G. Lyapin, and H. Saitoh, Phys. Rev. Lett. **105**, 115701 (2010).

[8] G. Carini, Jr., E. Gilioli, G. Tripodo, and C. Vasi, Phys. Rev. B **84**, 024207 (2011).

[9] G. Carini Jr, G. Carini, G. Tripodo, G. Di Marco, and E. Gilioli, Phys. Rev. B **85**, 094201 (2012).

[10] A. C. Wright, G. Dalba, F. Rocca, and N. M. Vedischcheva, Phys. Chem. Glasses: Eur. J. Glass Sci. Technol. B **51**, 233 (2010).

[11] A. I. Chumakov, G. Monaco, A. Fontana, A. Bosak, R. P. Hermann, D. Bessas, B. Wehinger, W. A. Crichton, M. Krisch, R. Rüffer *et al.*, Phys. Rev. Lett. **112**, 025502 (2014).

[12] G. Carini, Jr., G. Carini, G. D'Angelo, G. Tripodo, G. Di Marco, C. Vasi, and E. Gilioli, Phys. Rev. Lett. **111**, 245502 (2013).

[13] D. Fioretto and F. Scarponi, Mater. Sci. Eng. A **521**, 243 (2009).

[14] *CRC Handbook of Chemistry and Physics*, 70th ed., edited by R. C. Weast (CRC Press, Boca Raton, FL, 1980).

[15] G. E. Gurr, P. W. Mongotmery, C. D. Knutson, and B. T. Gorres, Acta Cryst. B **26**, 906 (1970).

[16] The internal friction is defined as $Q^{-1} = 0.23\frac{\alpha_{\mathrm{db}} V}{\omega}$, where α_{db} is the acoustic attenuation in db/cm, V the sound velocity, and ω the angular frequency of ultrasonic waves.

[17] K. S. Gilroy and W. A. Phillips, Philos. Mag. B **43**, 735 (1981).

[18] A. Akhiezer, J. Phys. (USSR) **1**, 277 (1939).

[19] J. P. Bonnet, J. Non-Cryst. Solids **127**, 227 (1991).

[20] H. J. Maris, in *Physical Acoustics*, edited by W. P. Mason and R. N. Thurston (Academic Press, New York, 1971), Vol. VIII, p. 279.

[21] T. N. Claytor and R. J. Sladek, Phys. Rev. B **18**, 5842 (1978).

[22] F. L. Galeener and M. F. Thorpe, Phys. Rev. B **28**, 5802 (1983).

[23] K. A. Topp and D. G. Cahill, Z. Phys. B: Condens. Matter **101**, 235 (1996).

[24] H. E. Bommel and K. Dransfeld, Phys. Rev. **117**, 1245 (1960).

[25] E. Rat, M. Foret, G. Massiera, R. Vialla, M. Arai, R. Vacher, and E. Courtens, Phys. Rev. B **72**, 214204 (2005).